Polymer 51 (2010) 5592–5603

Contents lists available at ScienceDirect

Polymer

journal homepage: www.elsevier.com/locate/polymer

Six types of spherulite morphologies with polymorphic crystals in poly (heptamethylene terephthalate)

Kai Cheng Yen [a], Eamor M. Woo [a,*], Kohji Tashiro [b,**]

[a] Department of Chemical Engineering, National Cheng Kung University, Tainan, 701, Taiwan ROC
[b] Department of Future Industry-oriented Basic Science and Materials, Toyota Technological Institute, Tempaku, Nagoya 468-8511, Japan

ARTICLE INFO

Article history:
Received 19 May 2010
Received in revised form
30 August 2010
Accepted 14 September 2010
Available online 21 September 2010

Keywords:
Poly(heptamethylene terephthalate)
Polymorphism
Spherulites

ABSTRACT

Six types of spherulite morphologies packed with polymorphic crystals and their growth kinetics in melt-crystallized poly(heptamethylene terephthalate) (PHepT) were characterized using polarized-light optical microscopy (POM), Fourier transformed infrared microspectrometry (micro-FTIR), differential scanning calorimetry (DSC) and atomic-force microscopy (AFM). Two maximum melting temperatures (T_{max}), a higher 150 °C and a lower 110 °C, were used to melt the initially crystallized PHepT of either α- or β-crystal. The high T_{max} was enough to melt all nuclei, but the lower T_{max} was considered as near or slightly below the equilibrium melting temperatures of these two cells (if estimated by nonlinear methods). When crystallized at various T_c from these two T_{max}'s, PHepT can exhibit as many as six types of spherulites (Ring Type-I, -II, -III, Maltese-cross Type-1, -2, and -3) owing to different nucleations. Ring Type-I, Maltese-cross Type-1 and -3 spherulites are packed of the sole β-crystal, while Ring Type-II, -III and Maltese-cross Type-2 spherulites are attributed to the sole α-crystal. However, as the PHepT polymorphic cells are related to T_c, such correlations between the crystal cells and spherulite types (ring or ringless) cannot be ruled out to be a coincidence.

1. Introduction

Semicrystalline polymers exhibiting polymorphism and different types of spherulite morphology have been studied, such as in poly(vinylidene fluoride) (PVDF) [1–3], poly(1,4-butylene adipate) (PBA) [4–6], poly(hexamethylene terephthalate) (PHT) [7–9] and isotactic poly(1-butene) (i-PBu-1) [10–13]. Polymorphic behavior in PVDF, PBA, or PHT is dependent on crystallization temperature (T_c); besides, the spherulite morphology in these three polymers depends on not only T_c but also polymorphism [1,2,4–9]. Melt-crystallized PVDF shows the α-crystal at T_c lower than 160 °C; however, upon scanning from 160° to melt, the α-crystal transforms to the γ-crystal and the γ-crystal reaches a maximum amount at 170 °C then melts at temperature higher than 185 °C. In the temperature range of 160–185 °C, both the α- and γ-crystal of PVDF exist simultaneously [1], and two kinds of spherulites are observed, where one is ringless and the other is ring-banded. Kressler et al. [2] have characterized the correlation between the spherulite morphology and the polymorphism of PVDF using Fourier transformed infrared microspectroscopy (micro-FT-IR) and indicated that the ringed and ringless spherulites are attributed to the α-crystal and the γ-crystal, respectively. Spherulite morphology and polymorphic behavior in melt-crystallized poly(1,4-butylene adipate) (PBA) have also been well-studied. PBA shows the α-crystal (monoclinic) and β-crystal (orthorhombic) when crystallized at T_c higher than 31 °C and lower than 28 °C, respectively. At T_c lower than 28 °C, where only the β-crystal is crystallized, the spherulite morphology is highly crystallization temperature dependent. At T_c lower than 25 °C, PBA is crystallized into the Maltese-cross (ringless) spherulites, while at T_c = 26–28 °C, PBA exhibits the ringed ones. The mechanism in the formation of ring bands in melt-crystallized PBA at T_c = 28 °C has been recently reported [14], and the great change of the steepness in height is considered to be the dominant mechanism. Unlike the β-crystal produced at lower T_c (lower than 28 °C), PBA melt-crystallized at T_c higher than 31 °C exhibiting the α-crystal is packed into the Maltese-cross ringless spherulites independent on T_c [4,5].

PHT, an aryl-polyester with six methylene groups between two terephthalate groups, exhibits complex polymorphic behavior upon melt crystallization. PHT contains both the α- and β-crystals when melt-crystallized at T_c lower than 140 °C, whereas when T_c is higher than 140 °C, crystallized PHT contains only the β-crystal. Upon

* Corresponding author. Tel.: +866 6 275 7575; fax: +866 6 234 4496.
** Corresponding author.
E-mail addresses: emwoo@mail.ncku.edu.tw (E.M. Woo), ktashiro@toyota-ti.ac.jp (K. Tashiro).

0032-3861/$ – see front matter © 2010 Elsevier Ltd. All rights reserved.
doi:10.1016/j.polymer.2010.09.031

crystallization at $T_c = 100$ °C, PHT possesses mixed α- and β-crystal cells, and PHT can be crystallized into mixed morphologies composed of Maltese-cross ringless spherulites and dendrites. An earlier investigation has pointed out that there may be a correlation between the spherulite morphology and the polymorphism in PHT [7]. The normal Maltese-cross spherulites correspond to the α-crystal and the dendritic morphology is associated with the β-crystal. Apart from the effect of the crystallization temperature, polymorphic behavior in semicrystalline polymers is also influenced by crystallization condition, such as cold crystallization, melt crystallization, solvent-induced crystallization or presence of nucleating agent. Isotactic poly(1-butene) (iPB-1) is a polymorphous semicrystalline polyolefin exhibiting four types of crystals, form I, form I′, form II and form III [8]. Form I′ is crystallized from a certain dilute solution or in thin film at elevated temperature (150 °C, 5 days), while Form I, the most stable crystal form in iPB-1, is produced through transformation from Form II when kept at ambient temperature for long time. These four types of crystals in iPB-1 have been claimed to assume different spherulite morphology corresponding to each crystal form, in which the spherulites of Form I and -II are ringless and those of Form III are ring-banded [8].

Polymers mentioned above are all polymorphous and exhibit different spherulite morphology corresponding to each crystal form. In this study, poly(heptamethylene terephthalate) (PHepT) served as a model polymer to go further on investigations of the spherulite morphology of a polymorphous polymer. PHepT exhibits polymorphism (α- and β-crystal) in melt crystallization depending the crystallization temperature (T_c) and maximum melting temperature (T_{max}) [15–17]. When heated at a lower T_{max} (110 °C) containing some traces of α- or β-nuclei and quenched to T_c, the crystallized PHepT shows the sole α-crystal or the mixed $\alpha+\beta$ crystal, respectively. In contrast, when heated at a higher T_{max} (150 °C) and quenched to T_c, the crystallized PHepT is packed of the sole β- and α-crystal at T_c higher than 35 °C and lower than 25 °C, respectively. Although the polymorphic behavior in PHepT has been well analyzed and proven [15], the corresponding spherulite morphology in association with each of these two crystal forms (α- or β-crystal) has yet to be characterized. The lower T_{max} (110 °C) might be superficially over the equilibrium melting temperatures of the α or β-crystal cells of PHepT (T_m °= 98 and 100.1 °C, linear Hoffman-Weeks extrapolation method) [18]. However, the conventional linear extrapolation procedures for obtaining the equilibrium melting temperatures of polymers might have underestimated the true equilibrium melting temperatures. The equilibrium melting temperatures of the α- and β-crystal according to the nonlinear Hoffman–Weeks method are 121 °C and 122.5 °C, respectively [18]. Thus, the reason of using $T_{max} = 110$ and 150 °C for melting the PHepT samples was based on the result of $T_{max} = 110$ °C being lower than and $T_{max} = 150$ °C being higher than T_m °= 121 °C – 122.5 °C (nonlinear method). By subjecting PHepT in thin-film forms to $T_{max} = 110$ or 150 °C, respectively, the spherulitic morphology and growth kinetics in melt-crystallized PHepT packed of either of α- or β-crystal or both crystal cells were characterized using polarized optical microscopy (POM), atomic-force microscopy (AFM), Fourier transformed infrared microspectrometry (micro-FTIR) and differential scanning calorimetry (DSC) in order to reveal the exact natures of multiple types of spherulites packed with polymorphic crystal cells.

2. Experimental

2.1. Materials

Poly(heptamethylene terephthalate) (PHepT) was not commercially available and was synthesized in-house using a catalyst (butyl titanate) by following the method described earlier in the literature [19]. Characterizations showed basic physical data for PHepT, whose $T_g = -1.6$ °C, $T_m = 96$ °C, $M_w = 37{,}500$ g/mol (gel permeation chromatography, GPC, Waters), and polydispersity index (PDI) = 1.7 (GPC).

PHepT was heated to a maximum temperature (T_{max}), held to ensure equilibrium, then quenched rapidly to a crystallization temperature (T_c) for various times to ensure full crystallinity. Two maximum melting temperatures (T_{max}), 150 °C and 110 °C, were used to melt the initially crystallized PHepT crystals of either α- or β-crystal. PHepT is polymorphic and samples could be prepared to contain solely α or β-type crystal, prior to being subjected to heating to the prescribed T_{max}. The higher T_{max} (150 °C) was capable of erasing all prior nuclei, and upon crystallization at T_c higher than 35 °C, only β-crystal was found [15]. Samples treated at $T_{max} = 150$ °C are coded as **PHePT-150**.The other T_{max} (110 °C) would permit presence of trace nuclei of either α- or β-crystal, depending on the crystal forms prior to heating to T_{max}. PHepT originally of β-form was heated at $T_{max} = 110$ °C so that they contained β-form nuclei at this T_{max}; upon crystallization at any T_c by quenching from $T_{max} = 110$ °C would lead to crystals of both α- and β-forms. PHepT samples treated at $T_{max} = 110$ °C and crystallized with β-nuclei are coded as PHepT-110β. On the other hand, PHepT originally of α-form was heated at same $T_{max} = 110$ °C so that they contained α-form nuclei at this T_{max}; upon crystallization at any T_c by quenching from $T_{max} = 110$ °C would lead to only α-crystal. Samples treated at $T_{max} = 110$ °C and crystallized with α-nuclei are coded as PHepT-110α These crystallization procedures were performed either in DSC cells or on microscopic hot stages, both with precision temperature control, depending on characterization to be followed.

2.2. Apparatus

2.2.1. Differential scanning calorimetry (DSC)

DSC measurements were made in a Perkin–Elmer DSC-Diamond equipped with a mechanical intracooler under dry nitrogen purge. Temperature and heat flow calibrations at different heating rates were done using indium and zinc. Considerably slow heating rates of 0.1 °C/min and 0.5 °C/min were used to completely separate the overlapped melting peaks of the α- and β-crystals.

2.2.2. Fourier transform infrared microspectroscopy (micro-FTIR)

Micro-FTIR measurements were performed at a resolution of 2 cm^{-1} on a Varian 600 UMA microscope with a Varian 3100 FTIR spectrometer equipped with an MCT detector. The lateral resolution of micro-FTIR is 11 μm × 11 μm. Samples for micro-IR measurements were thin PHepT films of 4–5 μm thickness, which were prepared by dissolving the polymer in chloroform (~2 wt%) and cast onto KBr pellets at ambient temperature. The films on KBr pellets were dried in vacuum at 40 °C for 2 days to remove the residual solvent.

2.2.3. Polarizing-light optical microscopy (POM)

A Nikon Optiphot-2 polarized-light optical microscope (POM) equipped with a charge-coupled device (CCD) digital camera and a Linkam THMS-6000 microscopic heating stage with TP-92 temperature programmer was used to observe the crystal morphology of the isothermally crystallized samples. The CCD equipped with automated image software was used to capture the morphology of the isothermally crystallized samples at preset time intervals. Thin-films specimens for POM were sandwiched between two glass slides.

2.2.4. Atomic-force microscopy (AFM)

AFM characterizations were performed in intermittent tapping mode (Caliber, Veeco-DI Crop., USA), using a silicon tip ($\nu = 70$ kHz,

r = 10 nm). Sample preparation is similar with that for POM observation.

3. Results and discussion

Polymorphic behavior in melt-crystallized PHepT (α- or β-crystal) depends on maximum melting temperature (T_{max}) and crystallization temperature (T_c) [15]. The thin-film samples exhibiting the spherulites packed of the sole β-, α- or mixed α+β-crystal were prepared using the methods mentioned earlier and observed using POM. Fig. 1 shows the POM micrographs for the spherulite morphology of melt-crystallized PHepT-150 at T_c = 40–75 °C packed of only β-crystal cell. With T_{max} = 150 °C, only the β-crystal cell is present in PHepT when crystallized at T_c higher than 35 °C. Upon crystallization at T_c = 50–65 °C, PHepT exhibits mainly ringed spherulites with zig-zag bands and the ring spacing becomes wider with increasing T_c from 50 to 65 °C. By contrast, at T_c = 40 °C or T_c higher than 70 °C, PHepT exhibits ringless spherulites with Maltese-

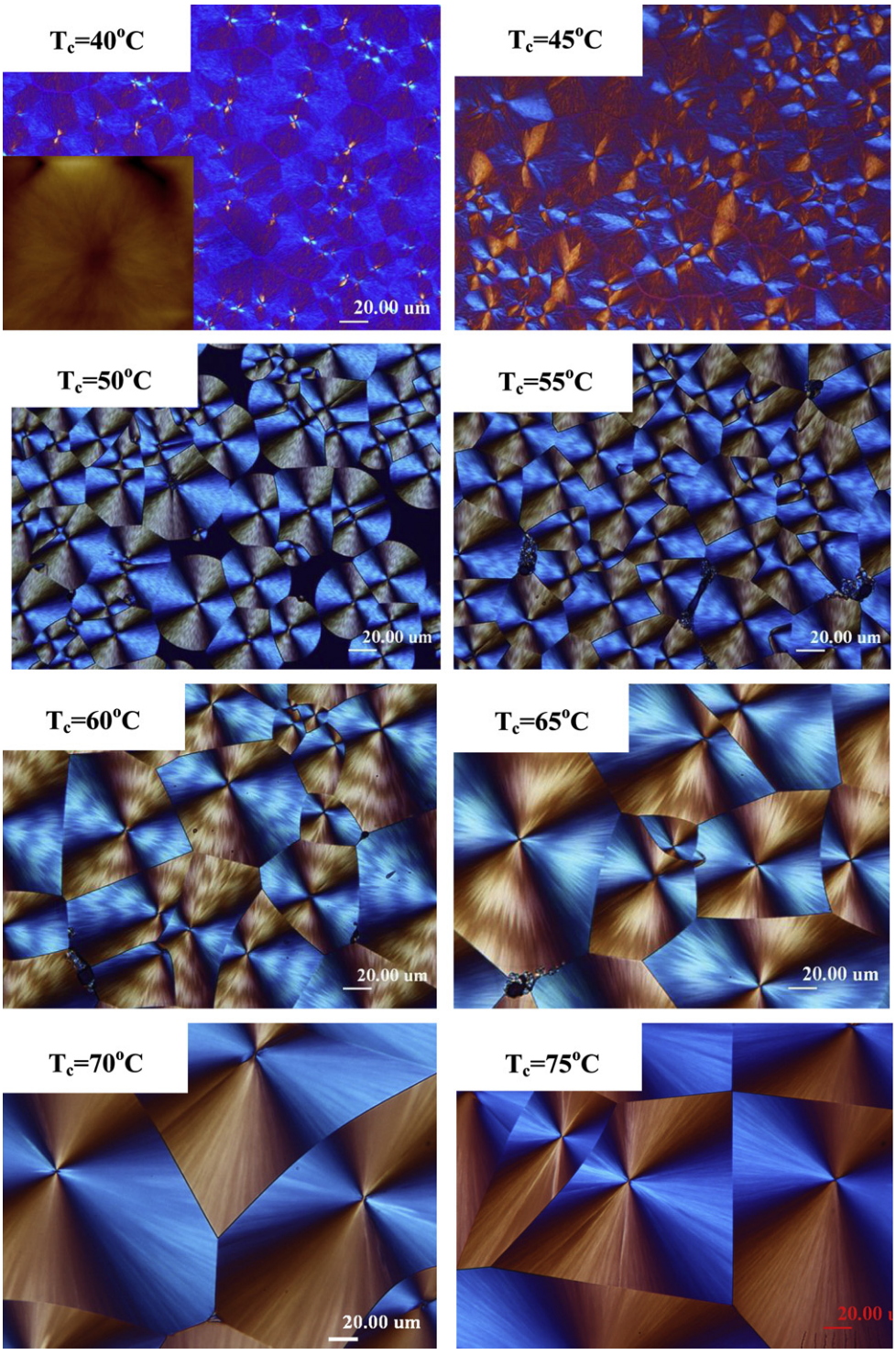

Fig. 1. POM micrographs of spherulite morphology in melt-crystallized PHepT-150 at T_c = 40–75 °C.Inset: AFM height image of spherulite in PHepT-150 crystallized at 40 °C.

cross patterns, in which the birefringence of the ringless spherulites crystallized at 40 °C is lower than that of the ringless spherulites crystallized at T_c higher than 70 °C. The AFM image of a much higher magnification than POM is shown as an inset in the POM micrograph for the PHepT spherulites crystallized at $T_c = 40$ °C, and the AFM micrograph manifests that the spherulites at this T_c are indeed ringless. At 45 °C, the spherulites are mixed fractions of both ringed and ringless due to morphological transition gradually from completely ringless to ring-banded with increasing T_c from 40 to 50 °C.

Fig. 2 shows the plot of the spherulite growth rates in melt-crystallized PHepT-150 versus T_c. The spherulite growth rate was determined from the slope of the plot in the spherulite radius versus time at each T_c (not shown for brevity). The figure shows that the spherulite growth rate increases from $T_c = 40$ °C and reaches a maximum at $T_c = 55$ °C then decreases with further increasing T_c to 80 °C. The radial growth rate, G, can be described by the equation $G = G_0 e^{\Delta E/RT} e^{-\Delta F^*/RT}$ [20–22], where ΔF^* is the free energy of creating a surface nucleus of critical size, and ΔE is the activation free energy for a chain crossing the barrier to crystal. This equation allows the temperature dependence of spherulite growth rates to be understood in terms of two competing processes, with one being the molecular transportation rate in the melt and the other the nucleation rate. The molecular transportation rate increases with increasing T_c, while the nucleation rate decreases with increasing T_c. Between these two extremes, the growth rate passes through a maximum where these two factors are approximately equal in magnitude. Thus, this figure shows a bell-shaped curve with a maximum at $T_c = 55$ °C.

The well-established Lauritzen–Hoffman theory was subsequently applied to further analyze the spherulite growth kinetics in melt-crystallized PHepT. The expression for the crystallization process can be described in terms of the following equation [23,24]:

$$G = G_0 \exp\left[\frac{-U^*}{R(T_c - T_\infty)}\right] \exp\left[\frac{-K_g}{fT_c\Delta T}\right] \quad (1)$$

where G is the radial growth rate and G_0 is an overall constant factor depending on the molecular weight. The first exponential term in Eq. (1) accounts for the process of the transport of molecular segments to the crystalline surface (transport term), where U^* is the activation energy, R is the gas constant, T_c is the crystallization temperature, and T_∞ generally defined as $T_g - 30$ K, is the temperature at which the transport of segments across the liquid–solid interface becomes infinitely slow. The second exponential term (nucleation term) is a measure of the probability of creating a thermodynamically stable secondary surface nucleus, where ΔT is the degree of under-cooling ($\Delta T = T_m^\circ - T_c$), and f is the correction factor for the effect of temperature on the heat of fusion, taken as $2T_c/T_m^\circ + T_c$. Eq. (1) is usually re-written in a logarithmic form:

$$\log G + \left[\frac{U^*}{R(T_c - T_\infty)}\right] = \log G_0 + \left[\frac{-K_g}{2.303fT_c\Delta T}\right] \quad (2)$$

The spherulite growth rate (G) at each T_c shown in Fig. 2 was then introduced to eq. (2) and by plotting the left side of eq. (2) versus $1/fT_c\Delta T$, the value of $K_g(i)$ (i = the crystallization regime, I, II, or III) was determined from the slope of the straight line fitted in each regime.

Fig. 3 shows the Lauritzen–Hoffman plot in melt-crystallized PHepT-150 at $T_c = 40$–80 °C with $U^* = 1250$ cal/mol and $T_m^\circ = 100.1$ °C as determined using the linear Hoffman–Weeks method [18]. Spherulites are mainly packed of sole β-crystals. There is a regime transition from regime III to regime II at 63–65 °C with increasing T_c and the value of $K_g(\mathrm{III})/K_g(\mathrm{II})$ is 2.02, which is considerably close to the theoretical value corresponding to transition from regime III to regime II [24]. Insets shown in this figure are the POM micrographs of the spherulites corresponding to each T_c in regimes. The normal Maltese-cross spherulites are crystallized at the lower T_c region (40 °C) within regime III and the higher temperature region within regime II (70–80 °C). These two temperature regions (40 °C and 70–80 °C) are at the extreme ends of the temperature range. In contrast, the ring-banded spherulites are crystallized at $T_c = 50$–65 °C, which covers most of regime III (50–65 °C). Within Regime III, the β-crystal spherulites are all ring-banded (except for very low T_c near 40 °C), with the inter-ring spacing increasing with T_c from 50 to 65 °C. Note, however, for very low T_c, the spherulites are tiny and any ring bands, even if present, may be too thin (much less than one micron) for POM resolution. The crossover point of the regime transition from III to II is approximately located between 63 and 65 °C (with some experimental deviation). At the regime transition $T_c = 65$ °C or higher T_c,

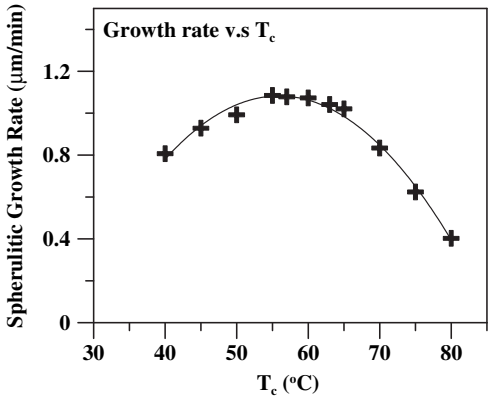

Fig. 2. Growth rates versus T_c in melt-crystallized PHepT-150 at $T_c = 40$–80 °C for β-crystal spherulites.

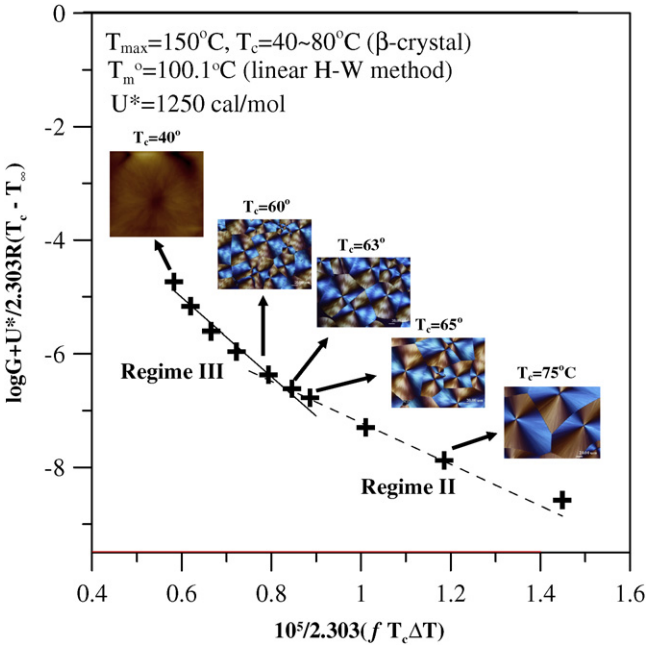

Fig. 3. Lauritzen–Hoffman plot in melt-crystallized PHepT-150 at $T_c = 40$–80 °C packed of sole β-crystal with U* = 1250 cal/mol. Insets: corresponding spherulite morphology at each T_c.

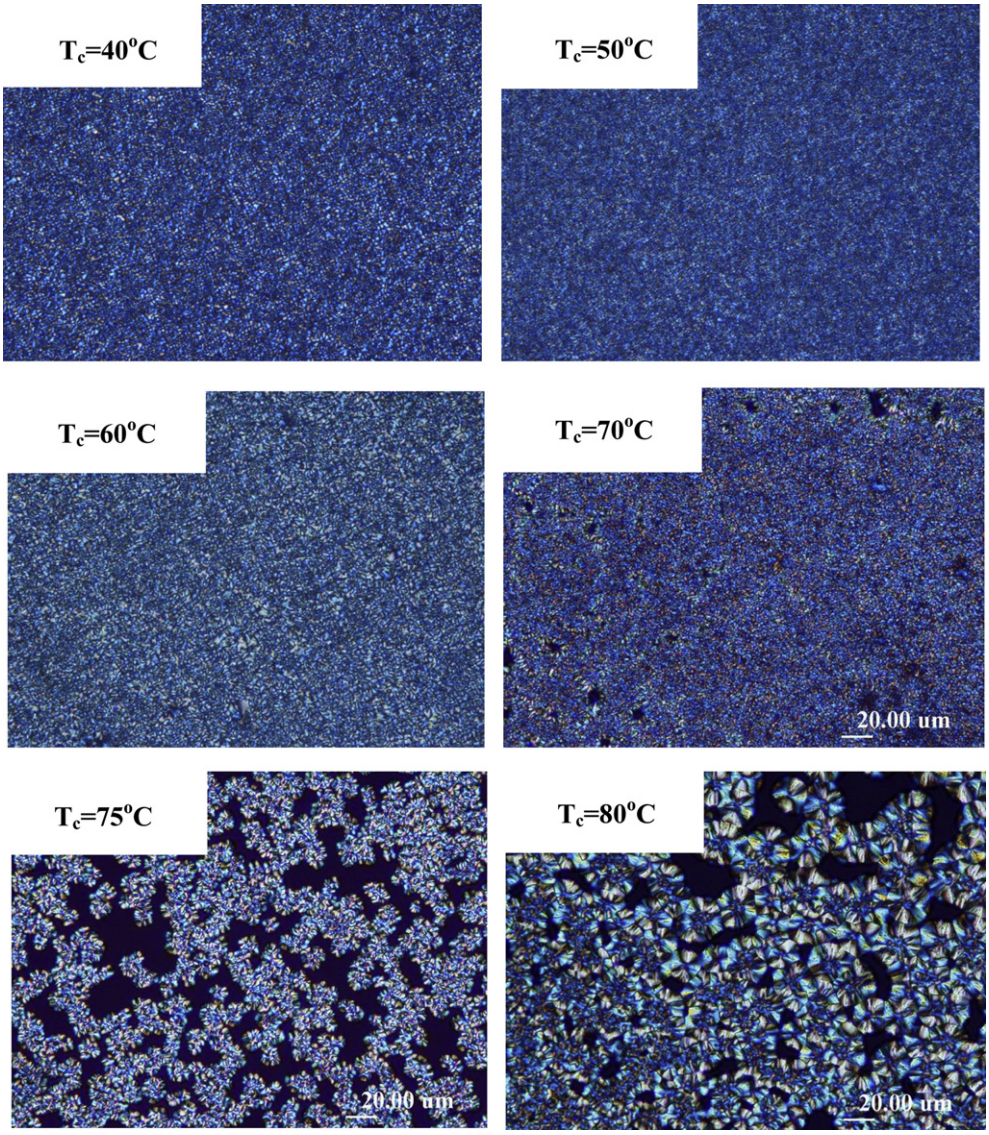

Fig. 4. POM micrographs of spherulite morphology in melt-crystallized PHepT-110α at T_c = 40–80 °C.

there is change in the β-crystal spherulites from ring-banded to ringless Maltese-cross types.

Other aryl-polyesters such as poly(trimethylene terephthalate) (PTT) [25] and poly(octamethylene terephthalate) (POT) [26] also show interesting correlations between the regime transition behavior and the spherulite morphology changes. Melt-crystallized PTT shows regime transitions from III→II→I accompanied by a morphological change from non-banded (Regime III) to ring-banded (Regime II) and then to axialite-like (i.e., dendritic) morphology (Regime I) with increasing T_c from 170 to 220 °C [25]. By comparison, POT shows only two regimes with transition from regime III to regime II accompanied by the morphological change from the ringed spherulites with regular ring-band patterns to dendritic spherulites with irregular zig-zag bands [26]. Extremely slow growth, especially at high T_c in Regime I, usually does not lead to ring bands, but leads to dendrites of straight lamellae or highly zig-zag ring bands that can hardly be classified as ordered rings. On the other extreme, the extremely fast growth at very low T_c end of regime III leads to tiny small spherulites that cannot be discerned for ring bands by POM (not POM-recognizable). However, it has been discovered that the extremely small spherulites crystallized at low T_c actually exhibit thin ring bands in poly(octamethylene terephthalate) beyond POM resolution but well-resolved by SEM [26]. Additional examples for such universality of regime transitions with spherulitic morphology changes are abundant. In addition, regular and orderly ring-banded spherulites in Regime III are found in the miscible blends of poly(ε-caprolactone) (PCL) with several different amorphous polymers such as poly(phenyl methacrylate) or poly(benzyl methacrylate), while crystallization in Regime II leads to highly dendritic spherulites with hardly recognized zig-zag rings [27]. Neat PCL may be different from its miscible blends with amorphous polymers and can be considered as an exception, as the neat PCL exhibits disordered and insignificant rings (barely ordered with zig-zag irregularity) only at a certain high T_c but ringless spherulites at most low T_c's. Thus, the morphology change corresponding to regime transition behavior is almost universal in many polymers including PHepT investigated in this study, even though some exceptions may exist. Note that this phenomenon of correlation may simply be a contingency of occurrence for many polymers because most polymers exhibit ring bands often in the low or sometimes intermediate T_c (i.e., near Regime III); but such correlations nevertheless can be verified in many proven cases.

The discussions above are on the spherulite morphology and growth kinetics in melt-crystallized PHepT-150 packed of the β-crystal only. By comparison, a lower T_{max} (110 °C) was applied to melt the original crystal (either the α- or β-crystal), and the samples were analyzed using POM on their spherulite morphology as well as the growth kinetics. Fig. 4 shows the POM micrographs of the spherulites in melt-crystallized PHepT-110α (with α-nuclei and crystallized into only α-form) at $T_c = 40–80$ °C. Under this thermal treatment, PHepT-110α exhibits the α-crystal only [15]. At $T_c = 40–70$ °C, tiny crystals are produced led by the heterogeneous nucleation mechanism which is attributed to presence of the traces of the α-nuclei when heated at $T_{max} = 110$ °C [24]. At higher T_c's (75 and 80 °C), small spherulites are observed owing to the lower nucleation density at higher T_c compared to that at lower T_c. However, detailed observations in the spherulite morphology packed of the α-crystal obtained under this thermal treatment are not feasible because the spherulites are too small.

In contrast to the sole α-crystal produced in melt-crystallized PHepT-110α, PHepT-110β is crystallized into both the α- and β-crystal at all T_c's [15]. It was thus of interest to compare the spherulite morphology in melt-crystallized PHepT packed of the mixed α- and β-crystal. Fig. 5(A) and (B) show the POM and AFM micrographs of the spherulites in PHepT-110β melt-crystallized at 40 °C, where graph-A and -B were focused on nearly the same area. Spherulites as observed under POM (graph-A) are of two different types differentiated by the birefringence (brighter and darker). The crystallized PHepT-110β samples may contain both α- and β-forms. The brighter (with higher birefringence) and darker (with lower birefringence) spherulites are both ringless as viewed under POM observation. Due to the limited resolution of POM, AFM of greater magnifications was applied to reveal the morphology of both bright and dark spherulites. Graph-C shows the AFM height images zoomed-in at higher magnifications on both dark and bright spherulites that are ear-marked with a white dotted circle in graph-B. No ring-band patterns are observed in the dark spherulite, while some protruded lamellae are observed in the bright one. Graph-D shows AFM height image for the bright spherulite as shown in graph-C (enclosed with white dotted line) which displays that the protruded lamellae appear in the surface are irregularly arranged and no definite ringed morphology is formed. Thus, the bright and dark spherulites in PHepT-110β crystallized at 40 °C are both none ring-banded, and thus they are referred as Maltese-cross Type-1 and -2, respectively, and abbreviated as M1 and M2 types.

Poly(butylene terephthalate) (PBT) [28,29] and (POT) [26] have been reported to exhibit the dual types of spherulites under certain crystallization conditions. Upon nonisothermal crystallization from the molten state at an appropriate cooling rate, two types of spherulites are produced in PBT, where one exhibits an optical axis 45° to radius defined as the unusual spherulite and the other exhibits an optical axis along or perpendicular to the radius defined

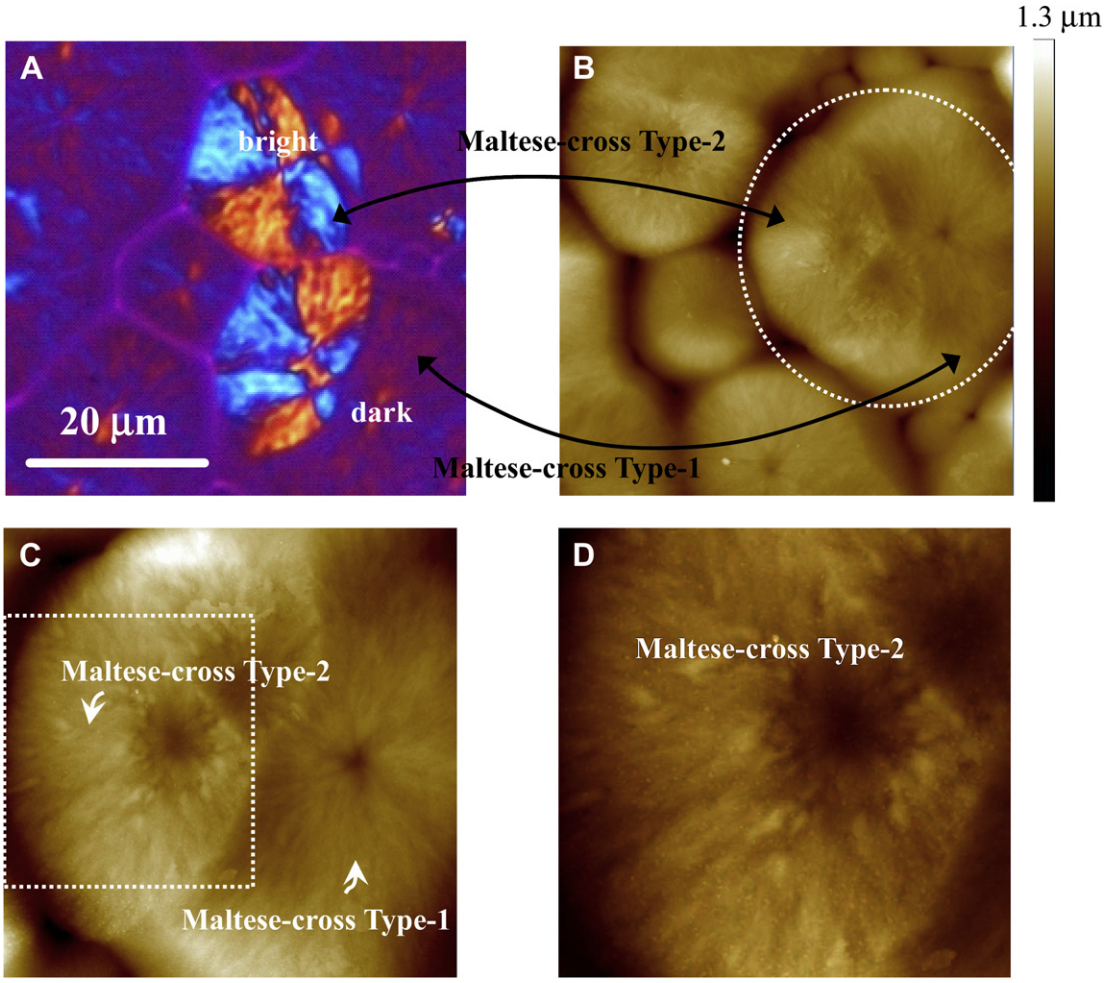

Fig. 5. (A) POM and (B) AFM micrographs (53.6 μm × 53.6 μm) of PHepT-110β melt-crystallized at 40 °C. AFM height zoomed-in images for (C) both bright and dark spherulites (27.6 μm × 27.6 μm) and (D) sole bright one (14 μm × 14 μm).

as the usual spherulite characterized using small-angle light scattering (SALS) technique and POM. Both the usual and unusual spherulites are ringless with the Maltese-cross patterns [28,29]. These two types of spherulites (usual and unusual) are of the same crystal unit cell (orthorhombic) but differ in the internal structure resulting in the different optical property. POT shows the dual types of spherulites upon melt crystallization. When T_{max} = 160 °C, ringed and ringless spherulites are simultaneously crystallized at T_c lower than 90 °C. However, when heated at T_{max} = 160 °C and quenched to T_c higher than 90 °C, only ringed spherulites can be crystallized. Moreover, when heated at a higher T_{max} = 240 °C, the ringed spherulites are solely crystallized at all T_c's. The ring-band patterns in the ringed spherulites of POT are temperature dependent, where the ringed spherulites exhibit regular ring bands and irregular zig-zag bands at T_c = 95–115 °C and T_c higher than 115 °C, respectively [26]. POT, similar to PBT, is packed with only one crystal cell form, which has been recently identified to be triclinic unit cell with dimensions of a = 4.560Å, b = 5.597Å, c = 18.703Å, α = 104.87°, β = 119.45° and γ = 100.32° [30]. These two polymers (PBT and POT) exhibiting dual types of spherulites upon crystallization are both of a monomorphic crystal; however, the spherulite morphology in PBT and POT differs significantly. Both dual types of spherulites of PBT are ringless but differ in optical property [28,29]. In contrast, those of POT are ringed and ringless, respectively [26].

Unlike POT and PBT, PHepT is a polymorphic polymer packed of the α-, β-crystal, or both crystals of various fractions depending on T_{max} and T_c, which further complicates the characterization on origins of the different types of spherulites in melt-crystallized PHepT. In a previous study [15], the individual peak-melting temperatures of the α- and β-crystal have been determined, where the peak-melting temperature of the α-crystal is 90 °C and that of the β-crystal is 96 °C upon scanning at 10 °C/min. Similarly, in this study, difference in the peak-melting temperature of the α- and β-crystals was used to analyze the correlations between the type of spherulites and crystal forms therein in the spherulites. Fig. 6 shows DSC thermograms upon scanning to (A) 110 °C and (B) 101 °C (scanning rate = 0.1 °C/min) of thin-film PHepT-110β samples (coated on micro-glass slide) crystallized at 40 °C exhibiting M1 and M2 spherulites, which are labeled previously in Fig. 5. The corresponding POM micrograph of the spherulite morphology in sample-(A) at 40 °C is shown as inset, where the darker one is M1 and the brighter one is M2 spherulite as defined earlier. Upon scanning from T_c (40 °C) to 110 °C, the DSC trace-(A) shows two melting peaks at 98 °C and 104 °C, which are attributed to the α- and β-crystal, respectively. The lower scanning rate (0.1 °C/min) leads to the shifts in the melting temperatures of the α- and β-crystal to higher temperatures compared to those scanned with scanning rate = 10 °C/min. The corresponding POM micrograph of the spherulite morphology of the 40°C-recrystallized sample is shown as inset, and only M1 spherulites and tiny crystals are observed. It indicates that upon heating to 101 °C to melt the α-crystal, M2 spherulites melt. In addition, upon re-crystallization at the original T_c, tiny crystals are produced because 101 °C is not high enough to erase all traces of the nuclei and thus leads to the heterogeneous nucleation and the crystallization of tiny crystals. Thus, a correlation can be concluded that M1 and M2 spherulites are attributed to the α- and β-crystals, respectively.

Fig. 7(A) shows POM micrographs of spherulites observed in PHepT-110β melt-crystallized at 50 °C. For samples crystallized at T_c = 50 °C, two types of spherulites are observed. One type is apparently ring-banded with zig-zag bands and termed as Ring Type-I (RI). The other type is roughly ringless but exhibits ring bands only in the Maltese-cross extinction region (enclosed as dotted lines) as viewed under POM. For better and higher resolution, AFM was used to characterize the ringless spherulites to reveal finer details. AFM micrographs for the type of POM-ringless spherulites are shown in Fig. 7(B). The larger magnification provided by AFM (about 2000× or higher) clearly reveals that these

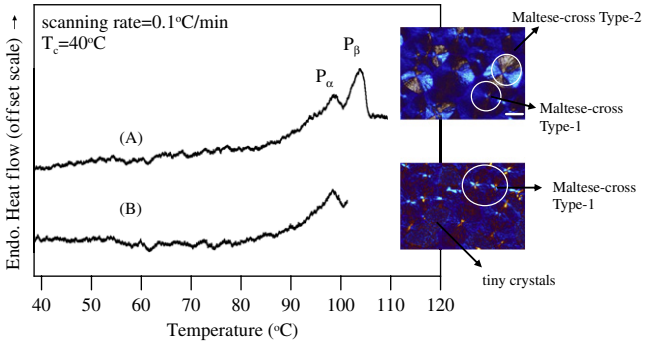

Fig. 6. DSC thermograms of thin-film samples of PHepT-110β exhibiting Maltese-cross Type-1 and -2 spherulites scanned to (A) 110 °C and (B) 101 °C (scanning rate = 0.1 °C/min). Inset-(top): Spherulite morphology of sample-(A) at 40 °C. Inset-(bottom): morphology of Sample-(B) scanned to 101 °C then re-crystallized at 40 °C.

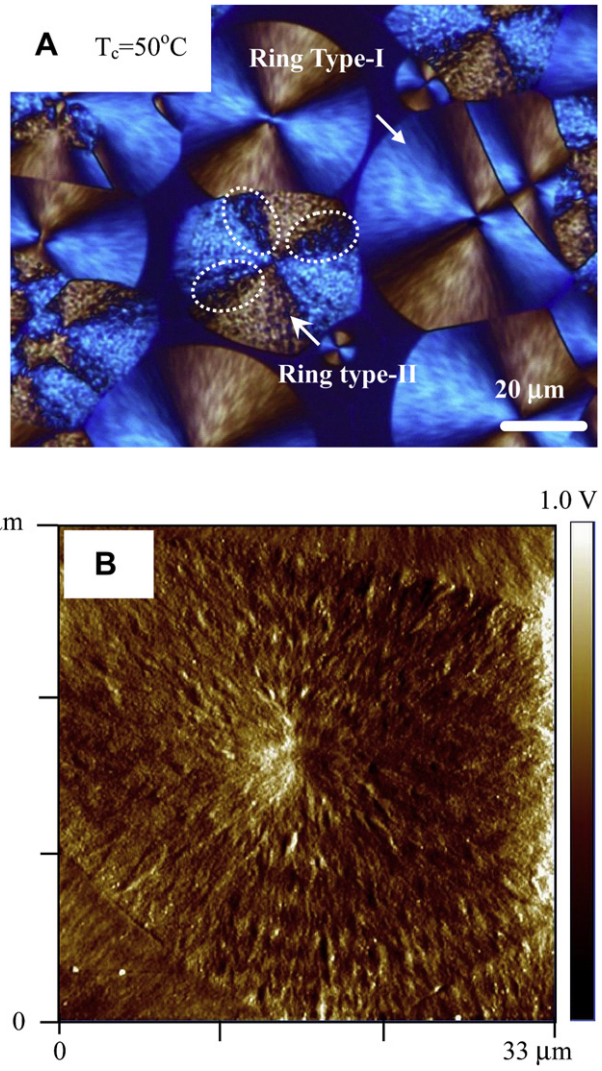

Fig. 7. (A) POM micrograph, (B) AFM (2000X) micrograph of Ring Type-II spherulite in PHepT-110β at T_c = 50.

ringless spherulites as viewed using POM for PHePT-110β crystallized at $T_c = 50$ °C actually contain an irregularly ring-band pattern. Thus, this type is re-named as Ring Type-II (abbreviated as RII).

Fig. 8 shows POM micrographs of PHepT-110β crystallized at 55–80 °C. At this temperature range, PHepT-110β also shows two types of spherulites. One type shows zig-zag ring bands same as those observed in RI spherulites and is classified to RI type. The other type shows narrow ring bands and the ring bands are more clearly observed in the Maltese-cross extinction region which is the characteristic of the RII spherulite and thus is classified to RII type spherulite. With increasing T_c to 65 °C, the inter-band spacing of both RI and RII spherulites increases and the ring-band patterns of RII become recognizable under POM observation. When T_c is increased from 65 to 70 °C, RII spherulites observed at 65 °C change from the ring-banded to eventually a ringless type at 70 °C. The ringless ones observed at 70 °C are named as Maltese-cross Type-3 and abbreviated as M3. With further increase of T_c to 75 °C, new double-ring-banded spherulites along with M3 spherulites are observed and the double-ring-banded ones are named as Ring Type-III (RIII spherulites).

Thermal analyses on the RI and RII spherulites were performed to identify their corresponding polymorphic crystals or lamellae. Fig. 9 shows DSC thermograms for thin-film PHepT-110β samples (sample spread as thin films and thermally treated on micro-glass slide) crystallized at 65 °C exhibiting RI and RII spherulites (as labeled previously) scanned to (A) 110 °C and (B) 101 °C (scanning rate = 0.5 °C/min). The corresponding inset POM micrograph of the spherulite morphology in sample-(A) at 65 °C shows RI and RII spherulites. Upon scanning from T_c (65 °C) to 110 °C, the DSC trace-(A) shows two melting peaks at 96 °C and 102 °C, attributed to endotherms of the α- and β-crystal, respectively. The lower scanning rate (0.5 °C/min) leads to up-shifting of the melting temperatures of the α- and β-crystal to higher temperatures in comparison to those scanned with rate of 10 °C/min. DSC trace-(B) shows one melting peak at 96 °C, attributed to melting of the α-crystal upon heating from T_c to 101 °C. After heating to 101 °C, the thin-film sample was quenched to the original T_c (=65 °C) and then allowed to recrystallize again for 1 h, prior to POM characterization. The corresponding POM micrograph of the spherulite morphology of the 65°C-recrystallized sample is shown as inset, and only RI

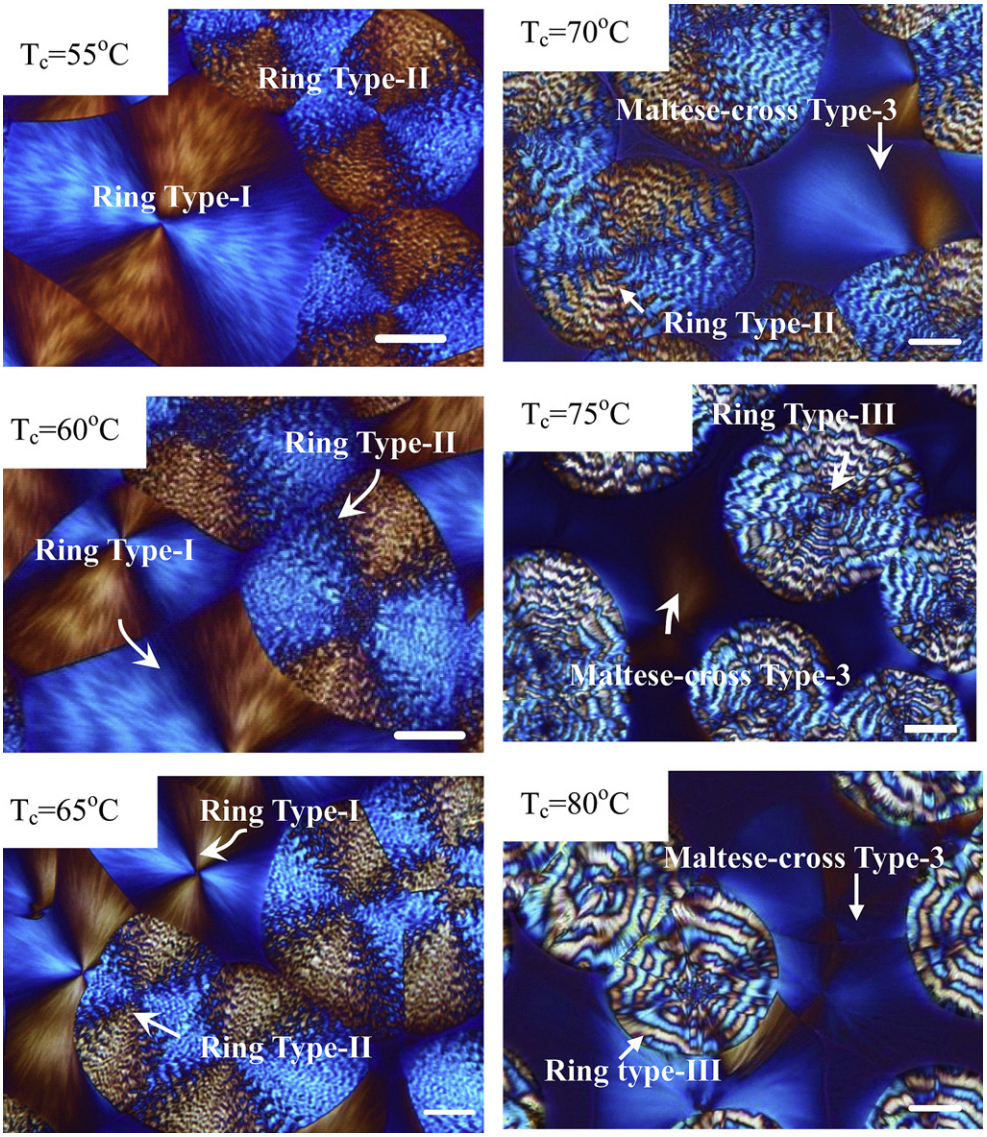

Fig. 8. POM micrographs of spherulite morphology in melt-crystallized PHepT-110β at T_c = 55–80 °C.

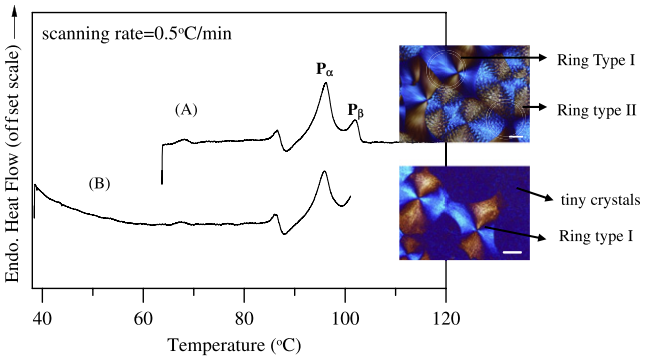

Fig. 9. DSC thermograms of thin-film samples of PHepT-110β exhibiting Ring Type-I and -II spherulites scanned to (A) 110 °C and (B) 101 °C (rate = 0.1 °C/min). Inset-top: morphology of Sample-(A) at 65 °C. Inset-bottom: morphology of Sample-(B) scanned to 101 °C then re-crystallized at 65 °C (Scale bar = 20 μm).

spherulites and tiny crystals are observed. Upon heating to 101 °C to melt the α-crystal, RII spherulites melt. In addition, after melting at 101 °C and upon re-crystallization at the original T_c, tiny crystals are produced because 101 °C is not high enough to erase all traces of the nuclei and thus these nuclei lead to heterogeneous nucleation into tiny crystals upon re-crystallization at T_c. Thus, it can be concluded that RI and RII spherulites are packed by the α- and β-crystals, respectively.

Correlations between the polymorphic behavior and RIII as well as M3 spherulites in PHepT-110β were analyzed by using Fourier transform infrared microspectrometry (micro-FTIR), because of the difficulty in resolving the overlapped melting peaks for the α- and β-crystals crystallized at this temperature range (75–80 °C) upon DSC scanning. Micro-FTIR provides a direct determination of the absorption spectra of the individual spherulite of micrometer scale. A previous study [15] has shown that the individual characteristic absorption bands correspond to the α- and β-crystal of PHepT. The corresponding IR absorption bands of the α-crystal are at 954, 1005, 1308 and 1476 cm^{-1}, and those of the β-crystal are at 950 and 1468 cm^{-1}.

Fig. 10 shows the micro-FTIR spectra in the range of (A) 900–1200 cm^{-1} and (B) 1250–1600 cm^{-1} of RIII and M3 spherulites of PHepT-110β. The spectra of RIII spherulite show the absorption bands at 954, 1005, 1308 and 1476 cm^{-1} which are associated with the α-crystal of PHepT. The spectra of the M3 spherulite show the absorption bands at 950 and 1468 cm^{-1} which are associated with the β-crystal of PHepT. Temperature-dependent micro-IR characterization on the α- and β-crystal spherulites in PHePT was attempted in a previous short communication [31], which led to some preliminary results. The temperatures at which disappearance of the crystalline IR absorbance bands for the α- and β-crystals took place were determined to be 98 and 106 °C, respectively. These two IR absorbance determined temperatures for the α- and β-crystal melting, respectively, match well with the melting temperatures of RIII and M3 spherulites determined using the temperature-controlled POM. Thus, by cross-referencing the micro-FTIR and POM morphology results, the predominant crystal cells in the RIII and M3 spherulites are likely packed with the α- and β-crystal, respectively. From these results above, the spherulite morphology of melt-crystallized PHepT can be influenced not only by crystallization temperature but also its polymorphic nature.

Note here that for this study on PHepT thin films, the collective techniques of micro-FTIR, POM and DSC characterizations were considered as the best choices for furnishing necessary evidence for correlating the crystal types and spherulite morphologies, rather than analysis based on the wide-angle X-ray (WAXD) technique

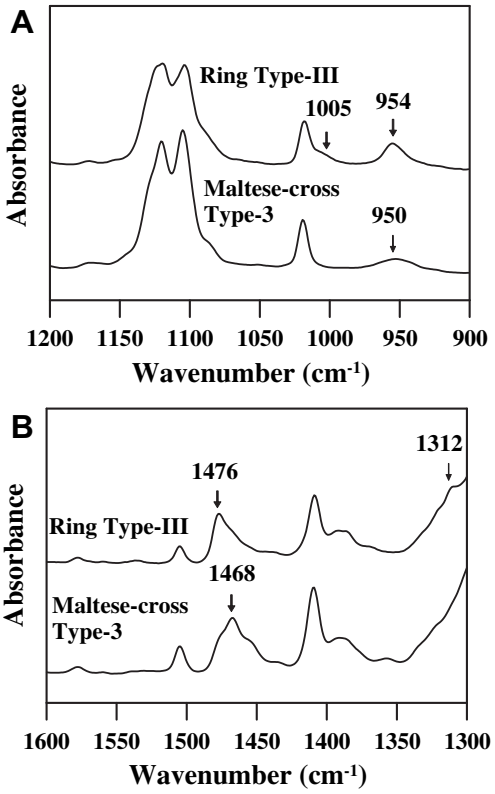

Fig. 10. Micro-FTIR spectra of Ring Type-III and Maltese-cross Type-3 spherulites in range of (A) 900–1200 cm^{-1} and (B) 1300–1600 cm^{-1}.

with temperature variation. To perform WAXD on micron-size spherulites in samples, it requires two fundamental fulfillments: (1) the X-ray beam size must be focused or narrowed to a few microns, and (2) the samples cannot be in thin films and have to be in bulk forms for sufficient X-ray signal intensity. However, when film thickness of samples is increased to thick or bulk forms, the crystallized spherulites in the PHepT bulks are no longer the same or comparable as those crystallized in thin films. More critically, different spherulite types in thick bulk polymers may be overlapped or stacked one on another, and the micro X-ray beam penetrates not a single type of spherulites, but goes through multiple layers of different spherulite types stacked in the bulk samples. Furthermore, it is critical that the temperature control accuracy should be precise in all techniques for meaningful comparisons, as the temperature accuracy and rapid stabilization of samples were critically important in the issues of crystal morphology addressed in this study. The three collective analytical tools used in this study, DSC, micro-FTIR, and POM, had temperature control precise enough and quick temperature stabilization for thin-film samples on substrates; by comparison, temperature control of X-ray temperature variation instrument was regarded to be more difficult, and rapid cooling or stabilization at intended set temperatures was rather slow.

PHepT-110β samples can be crystallized into co-existing α-crystal spherulites and β-crystal spherulites. The α-crystal spherulites in the PHepT-110β samples can assume different patterns depending on T_c. Fig. 11 shows evolution of spherulite morphology for the α-spherulites in the PHepT-110β samples transforming from ringless to ring-banded patterns upon crystallization at increasing T_c from 40 to 80 °C. Upon crystallization at a low T_c = 40 °C, the α-crystal spherulites exhibit a ringless type (M2 spherulite). Upon crystallization at T_c higher than 50 °C, the α-crystal spherulites in PHepT exhibit an

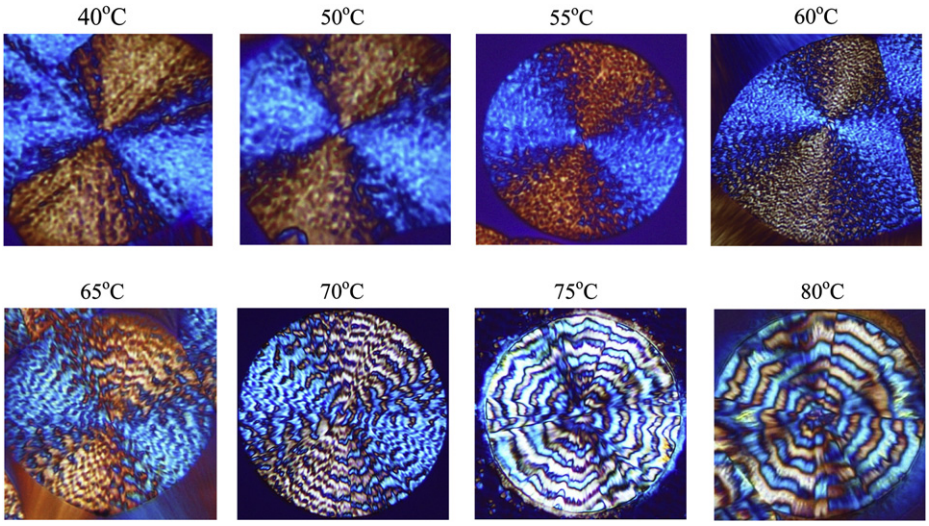

Fig. 11. POM micrographs of α-crystal spherulites at T_c = 40–80 °C.

irregularly ring-banded pattern (RII) at T_c = 50–70 °C. At increasing T_c from 50 to 70 °C, the ring bands on the arms of Maltese-cross are more distinct and more widely spaced than those between the Maltese-cross extinction arms. The spherulite morphology at further higher T_c becomes increasingly different in the ring-band patterns. Upon crystallization at T_c higher than 75 °C, the α-crystal spherulites are all double-ring-banded (RIII) type. In general, the ring-band spacing in the ringed α-crystal spherulites steadily increases with increasing T_c from 50 to 80 °C.

Fig. 12 shows spherulite growth rates for the α-crystal spherulites in the PHepT-110β samples versus T_c at T_c = 30–75 °C. The spherulite growth rate increases from T_c = 30 °C and reaches a maximum at T_c = 50 °C and then decreases with further increase of T_c to 75 °C. By comparing the growth rates of the spherulites packed of the β-crystal in melt-crystallized PHepT-150 as shown earlier in Fig. 2 with those of the α-crystal shown in this figure, the former ones are slightly higher than the later ones at all T_c's. The spherulite growth rates of the β-crystal spherulites crystallized in PHepT-110β are same as those determined in the β-crystal spherulites observed in PHepT-150 at all T_c's, and thus are not discussed here for brevity.

The growth rates of α-spherulites in the PHepT-110β determined at T_c = 30–75 °C were then introduced into Eq. (2) to analyze the regime transition behavior. Fig. 13 shows a Lauritzen–Hoffman plot for the α-crystal spherulites in the PHepT-110β samples (containing sole α-crystal) according to Eq. (2), by applying T_m^o = 98.0 °C as determined from the linear Hoffman–Weeks method [22] with U^* = 1250 cal/mol. The insets shown in this figure are POM micrographs of the α-spherulite crystallized at various T_c. One regime transition from regime III to regime II with K_g(III)/K_g(II) = 2.04 occurs at T_c = 60 °C. However, the morphology of the α-spherulite in PHepT-110β transits from ringless to irregular ring-banded at 50 °C, and further changes from irregular ring-banded to double-ring-banded at 75 °C. It indicates that there is correlation between the regime transition behavior and morphological change of the α-spherulites in PHepT-110β. By comparison with the β-type spherulites discussed earlier, regime transition temperature from regime III to regime II for the α-crystal spherulites is slightly different at ~60 °C, instead of ~65 °C. For the α-type spherulites, the regime transition occurs at T_c = 60 °C or higher, and there is change in the spherulitic morphology from to ringless Maltese-cross (Regime III) to ring-banded types (Regime II).

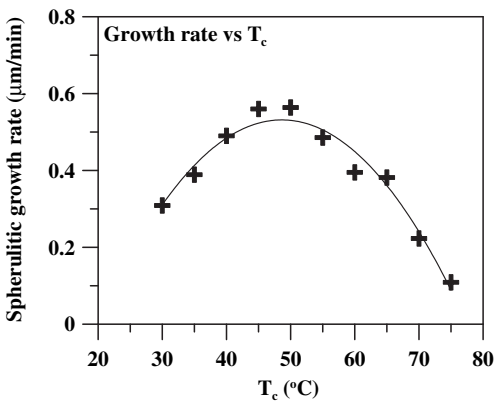

Fig. 12. Growth rates of α-crystal spherulites versus T_c range of 30–75 °C.

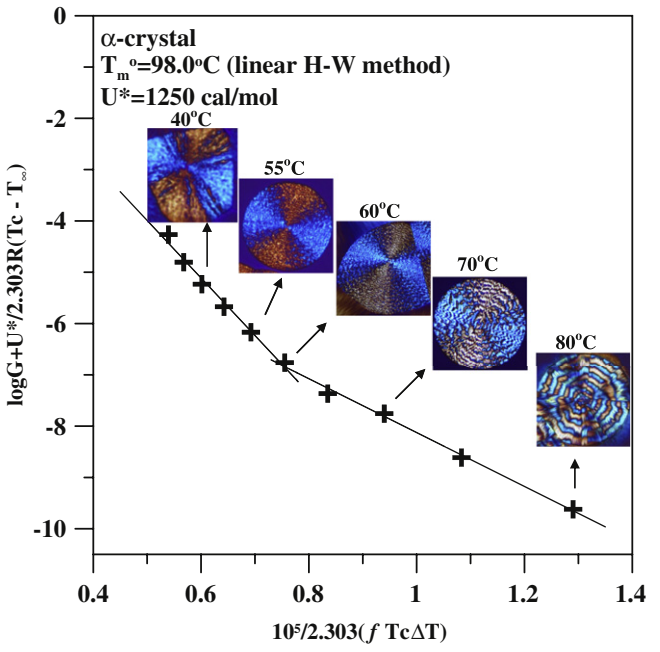

Fig. 13. Lauritzen–Hoffman plot in α-crystal spherulite of PHepT with U^* = 1250 cal/mol. Insets: corresponding spherulite morphology at each T_c.

Table 1
Six types of spherulites in PHepT.

Type of spherulite	Characteristic	Cells	Induction T_{max} and T_c
M1 	Low birefringence Maltese-cross (Ringless)	β	$T_{max} = 150\ ^\circ C$, $T_c = 40\ ^\circ C$ (without residual nuclei) $T_{max} = 110\ ^\circ C$, $T_c = 40\ ^\circ C$ (with residual β-nuclei)
M2 	(1) High birefringence (2) Some protruded lamellae irregularly appear in the surface (Ringless)	α	$T_{max} = 110\ ^\circ C$, $T_c = 40\ ^\circ C$ (with residual β-nuclei)
M3 	High birefringence Maltese-cross (Ringless)	β	$T_{max} = 150\ ^\circ C$, $T_c = 70–80\ ^\circ C$ (without residual nuclei) $T_{max} = 110\ ^\circ C$, $T_c = 70–80\ ^\circ C$ (with residual β-nuclei)
RI 	Zig-zag ring bands	β	$T_{max} = 150\ ^\circ C$, $T_c = 50–65\ ^\circ C$ (without residual nuclei) $T_{max} = 110\ ^\circ C$, $T_c = 50–65\ ^\circ C$ (with residual β-nuclei)
RII 	(1) Irregularly and narrowly ring-banded (2) Ring-band patterns are more apparent in Maltese-cross extinction region. AFM reveals ring bands in other areas.	α	$T_{max} = 110\ ^\circ C$, $T_c = 50–70\ ^\circ C$ (with residual β-nuclei)
RIII 	Regular double-ring-banded	α	$T_{max} = 110\ ^\circ C$, $T_c = 75–80\ ^\circ C$ (with residual β-nuclei)

For convenience of comparison, Table 1 summarizes the morphology, characteristics, crystallization conditions and crystal cells of six types of spherulites observed in melt-crystallized PHepT-110β and PHepT-150 samples. M1, M2 and M3 represent Maltese-cross Type-1, -2 and -3 spherulites and the morphologies are drawn in the upper three schemes of first column. The main morphological differences among M1, M2 and M3 spherulites are (1) M2 and M3 are of higher birefringence than that of M1, and (2) M2 spherulites show irregularly arranged lamellae protruding from surface as observed under AFM. On the other hand, RI, RII and RIII stand for Ring Type-I, -II and -III spherulites which are drawn in the lower three schemes of the first column. The main morphological differences among RI, RII and RIII spherulites are (1) RI spherulite exhibits zig-zag ring bands, (2) Ring bands in RII spherulites are irregular, narrow and more easily observed in the Maltese-cross extinction region, and (3) RIII spherulites are double-ring-banded. M1, M3 and RI spherulites are solely packed of the β-crystal and can be crystallized at their corresponding T_c's by quenching from two different conditions: (1) $T_{max} = 150\ ^\circ C$ erasing all prior nuclei and (2) $T_{max} = 110\ ^\circ C$ in presence of the residual β-nuclei. In contrast, M2, RII and RIII spherulites are packed of the sole α-crystal and can be crystallized at their corresponding T_c's only by quenching from $T_{max} = 110\ ^\circ C$ in presence of the residual β-nuclei.

4. Conclusion

Two maximum melting temperatures (T_{max}), 150 °C and 110 °C, were used to melt the initially crystallized PHepT crystals of either α- or β-crystal, which were chosen based on previously demonstrated nonlinear extrapolation leading to T_m° for the α- and β-crystal at about ~120 °C. The high T_{max} (150 °C) was enough to melt all nuclei, but the lower T_{max} (110 °C) was considered as near or slightly below the equilibrium melting temperatures of these crystal cells (as estimated by the nonlinear method). The higher T_{max} (150 °C) was capable of erasing all prior nuclei, while the lower T_{max} (110 °C) would permit presence of trace nuclei of either α- or β-crystal. Residual nuclei types (α- or β-crystal), whose presence was determined by T_{max}, are influential on the final spherulite and polymorphism morphologies of PHepT upon subsequent crystallization at T_c after quenching from T_{max}. When heated to the lower $T_{max} = 110\ ^\circ C$ that allows some residual α-crystal nuclei, upon quenching to T_c to crystallize, PHePT develops only tiny crystal spherulites packed solely of the α-crystal. However, if the initial

crystal nuclei is of the β-crystal type, the same T_{max} (110 °C) leads to crystallization of PHepT at various T_c's to exhibit as many as six types of different types of spherulites (Ring-banded Type-I, -II and -III, and Maltese-cross Type-1, -2 and -3) packed solely of either α- or β-crystals at various T_c. Note, however, that as the PHepT polymorphic cells are related to T_c, such correlations between the crystal cells and spherulite types (ring or ringless) cannot be ruled out to be a coincidence. Polymorphism distributes differently in the six different types of spherulites in PHepT. Ring-banded Type-I, Maltese-cross Type-1 and -3 spherulites are packed of only the β-crystal, whereas Ring-banded Type-II, -III and Maltese-cross Type-2 spherulites are packed of only the α-crystal cell.

The spherulitic growth rates of the α-crystal at all T_c's are slightly lower than those of the β-crystal. Regime transition temperatures from regime III to regime II for the α- and β-crystal spherulites are slightly different at ~60 and ~65 °C, respectively. Yet more striking differences are on the spherulite patterns. For the β-type spherulites, the regime transition occurs $T_c = 65$ °C or higher T_c, there is a general trend of change in the morphology from ring-banded (Regime III) to ringless Maltese-cross types (Regime II); conversely, for the α-type spherulites, the regime transition occurs at $T_c = 60$ °C or higher and there is an opposite trend of change in the spherulitic morphology from ringless Maltese-cross (Regime III) to ring-banded types (Regime II).

Acknowledgment

This work has been financially supported by a basic research grant (NSC-97-2221-E006-034-MY3) from Taiwan's *National Science Council* (NSC).

References

[1] Gregorio Jr R, Cestari MJ. Polym Sci Polym Phys Ed 1994;32:859.
[2] Kressler J, Schafer R, Thomann R. Appl Spectro 1998;52:1269.
[3] Gregorio Jr R, Capitão RC. J Mater Sci 2000;35:299.
[4] Wu MC, Woo EM. Polym Int 2005;54:1681.
[5] Woo EM, Yen KC, Wu MC. J Polym Sci Polym Phys 2008;46:892.
[6] Zhao L, Wang X, Li L, Gan Z. Polymer 2007;48:6152.
[7] Ghosh AK, Woo EM, Sun YS, Lee LT, Wu MC. Macromolecules 2005;38:4780.
[8] Hall IH, Ibrahim BA. Polymer 1982;23:805.
[9] Palmer A, Poulin-Dandurand S, Revd JF, Brisse F. Eur Polym J 1984;20:783.
[10] Lotz B, Thierry A. Macromolecules 2003;36:286.
[11] Marigo A, Marega C, Cecchin G, Collina G, Ferrara G. Eur Polym J 2000;36:131.
[12] Di Lorenzo ML, Righetti MC. Polymer 2008;49:1323.
[13] Jiang S, Duan Y, Li L, Yan D, Chen E, Yan S. Polymer 2004;45:6365.
[14] Andreas F, Woo EM, Lee LT, Chen YF, Förster S. Macromol Rapid Commun 2008;29:1322.
[15] Yen KC, Woo EM. Polymer 2008;50:662.
[16] Kawahara Y, Naruko S, Nakayama A, Wu MC, Woo EM, Tsuji MJ. Mater Sci 2009;44:2137.
[17] Kawahara Y, Naruko S, Nakayama A, Wu MC, Woo EM, Tsuji MJ. Mater Sci 2009;44:4705.
[18] Yen KC, Woo EM. J Polym Sci Polym Phys 2009;47:1839.
[19] Gilbert M, Hybart F. Polymer 1972;13:327.
[20] Sperling LH. Introduction to physical polymer science. New York: John Wiley & Sons; 2001.
[21] Wunderlich B. Macromolecular Physics, vol. 2. New York: Academic Press; 1976.
[22] Keith HD, Padden Jr FJ. J Appl Phys 1963;34:2409.
[23] Hoffman JD, Miller RL. Polymer 1997;38:3151.
[24] Hoffman JD, Miller RL. Macromolecules 1989;22:3038.
[25] Hong PD, Chung WT, Hsu CF. Polymer 2002;43:3335.
[26] Chen YF, Woo EM, Li SH. Langmuir 2008;24:11880.
[27] Chen YF, Woo EM. Colloid Polym Sci 2008;286:917.
[28] Stein RS, Misra MJ. Polym Sci Polym Phys 1980;13:327.
[29] Roche EJ, Stein RS, Thomas EL. J Polym Sci Polym Phys 1980;18:1145.
[30] Jeong YG, Lee SC, Shin KJ. Polym Sci Polym Phys 2009;47:276.
[31] Yen KC, Woo EM, Tashiro K. Macromol. Rapid Commun 2010;31:1343.